33RD INTERNATIONAL COSMIC RAY CONFERENCE, RIO DE JANEIRO 2013
THE ASTROPARTICLE PHYSICS CONFERENCE

On the correlation of the lateral and angular distributions of electrons in EAS

MARIA GILLER AND ANDRZEJ ŚMIAŁKOWSKI

University of Lodz, Faculty of Physics and Applied Informatics
Pomorska 149/153, 90-236 Lodz, Poland

maria.giller@kfd2.phys.uni.lodz.pl

Abstract: Using full simulations of EAS we study the dependence of the angular distribution of electrons at a given level of shower development on their distance from the shower axis. A parametrization of these distributions for electrons with fixed energies is given. We find a significant correlation of the electron radial angle and its lateral distance. This has an impact on the correct prediction of shower images in the Cherenkov light what is particularly important for reconstruction of showers with rather small incident angles.

Keywords: ultra high energy extensive air showers, Cherenkov light, shower reconstruction

1 Introduction

The motivation to undertake the present study has been a working out of a correct method for reconstructing the cascade curve of a shower from its optical images taken by fluorescence detectors of the highest energy cosmic ray arrays (such as the Pierre Auger Observatory, HiRes, Telescope Array). In particular, an instantaneous image of a nearby shower in the Cherenkov light depends on the three-dimensional lateral and angular distribution $f(\theta,r)$ of the emitting electrons at the observed level (see later). These distributions have not been found analytically as the bulk of electrons in a shower have energies of the order of the critical energy β of the medium; the analytical methods, however, work well for electron energies $E >> \beta$.
The advent of computers has made possible studying characteristics of EAS not available by analytical methods. Since we are interested in a dependence of the electron angular distributions at a given level of shower development on the distance from the shower axis we have to refer to shower simulations [1]. However, we think it would be instructive to present first some of the relevant analytical results concerning small-angle scattering of a charged relativistic particle propagating in matter.

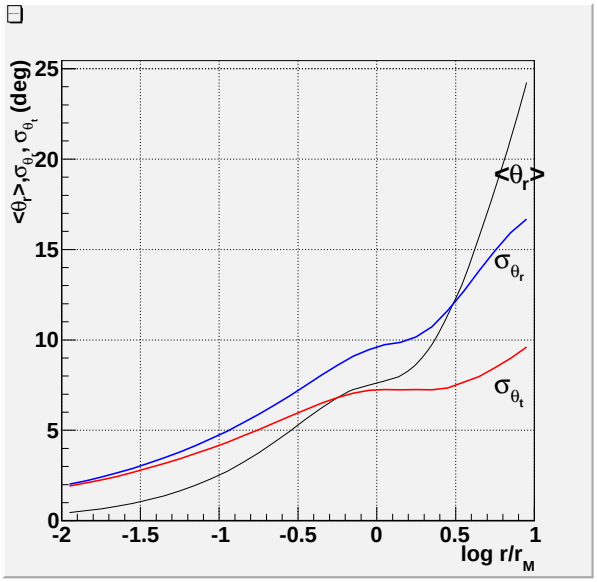

Figure 1: Average radial angle $< \theta_r >$, its dispersion σ_{θ_r} and the dispersion σ_{θ_t} of the tangential angle θ_t as function of the lateral distance r/r_M (in Molière units). Electron energies $E > 22$ MeV, $s = 0.95$.

2 Small-angle scattering

Let us consider a charged relativistic particle (electron) incident along the z-axis on a medium. We first assume that the thickness of the medium is such that the energy losses (whatever they may be) are negligible along the particle propagation. The next assumption is that the scattering angles in each particular Coulomb process are small and that the eventual angle $\theta(z)$ (i.e. after the particle traverses a final distance z) is small as well. One can write (and solve!) the so called diffusion equations for the two-dimensional distribution $W(\theta_x,x;z)$, where x,y are the axes perpendicular to z and θ_x is the projection of the angle θ on the x,z-plane [2]. The solutions are given in a form of a two-dimensional integral in a complex plane, but in the limit $z \to \infty$ we have obtained that

$$W(\theta_x,x;z) = \frac{1}{2\pi\sigma_{\theta_x}\sigma_x\sqrt{1-\kappa^2}} \quad \times \qquad (1)$$

$$\times \quad exp\Big[-\frac{1}{2(1-\kappa^2)}\Big(\frac{\theta_x^2}{\sigma_{\theta_x^2}} - 2\kappa\cdot\frac{\theta_x\cdot x}{\sigma_{\theta_x}\cdot\sigma_x} + \frac{x^2}{\sigma_x^2}\Big)\Big]$$

where κ is the correlation coefficient between the two variables θ_x and x. We derive that $\kappa = \sqrt{3}/2 \cong 0.866$. Thus, in the considered case, the lateral distance x and the angle θ_x in the x,z plane are strongly correlated. The value of κ does not depend on the details of the scattering, hence it is independent of the particle energy.
The distribution (1) integrated over x (over θ_x) gives a Gaussian distribution of θ_x (of x), as should be expected, with the mean $= 0$ and the variance σ_{θ_x} equal to the variance in a single scattering multiplied by the number of the scatterings.
In the process of the propagation through the medium the particle (electron) loses, however, energy. On the assumption that the scattering is due to the Coulomb forces we have that

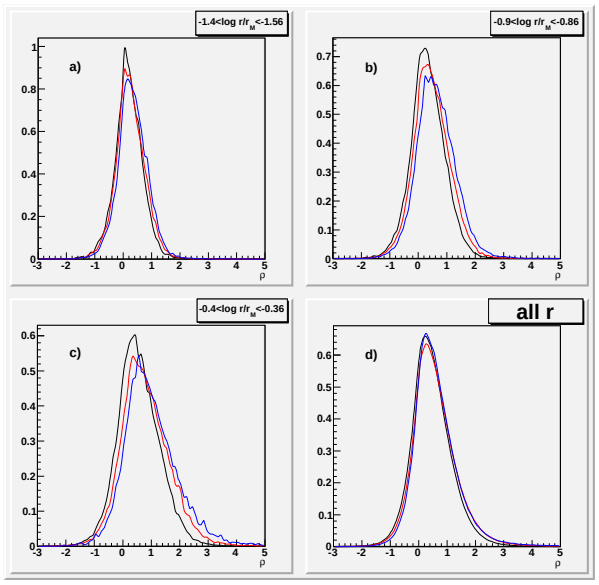

Figure 2: Distributions of $\rho = \theta_r \cdot E^{0.73}$ (θ in degrees, E in GeV) for three electron energies E =22 MeV (black curve), 67 MeV (red) and 200 MeV (blue) (from bins $(E, 1.1E)$); a) $-1.4 < log\frac{r}{r_M} = y < -1.56$, b) $-0.9 < y < -0.86$, c) $-0.4 < y < -0.36$, d) all distances.

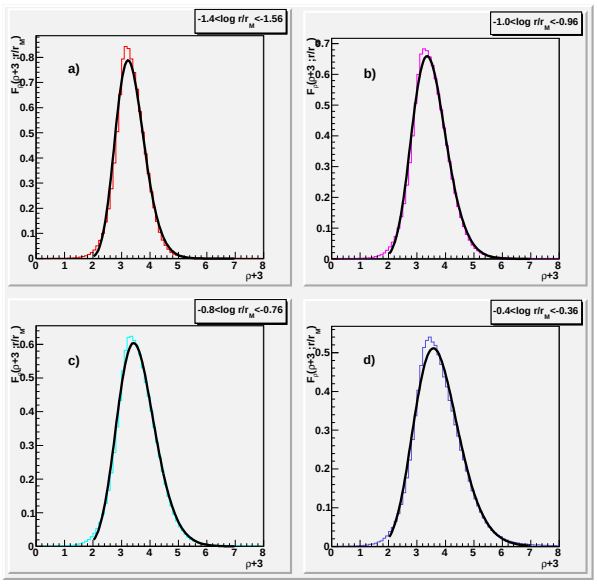

Figure 3: Distributions $F_\rho(\rho+3; r/r_M)$ (histograms) and fits with Nishimura-Kamata functions (lines) for four distance bins: a) $-1.4 < y < -1.56$, b) $-1.0 < y < -0.96$, c) $-0.8 < y < -0.76$, d) $-0.4 < y < -0.36$

$$< \theta_x^2(z) >= \int_0^z \left[\frac{E_s}{E(z')}\right]^2 \frac{dz'}{X_0} \qquad (2)$$

where $< \theta_x^2(z) >$ is the electron mean square angle (in the x,z- plane) at depth z, $E_s \cong 15$ MeV, $E(z')$ is the electron energy at depth z' and X_0 is the cascade unit of the medium. For the mean square lateral distance we obtain

$$< x^2(z) >= \int_0^z (z-z')^2 \left[\frac{E_s}{E(z')}\right]^2 \frac{dz'}{X_0} \qquad (3)$$

Since the correlation coefficient between θ_x and x does not depend on the electron energy it should be the same at any depth z. It is then natural to guess that, allowing for the energy losses, the two-dimensional distribution $W(\theta_x, x; z)$ should have the same form as that in (1), where (4) $\sigma^2_{\theta_x} =< \theta_x^2(z) >$ and $\sigma^2_x =< x^2(z) >$. Indeed, this function does fulfil the diffusion equation.

3 Angular and lateral distribution of electrons in EAS

In the extensive air shower, however, the situation is a little different. Let us consider electrons with a fixed energy E at some particular level of shower development. When following one of them up its energy increases but at times its path changes into a photon path, and then again into that of an electron. Along a photon path the angle does not change but the lateral distance does. Thus , the correlation between them deteriorates. Moreover, the great grandparents of these electrons (with the fixed energy E) have a distribution of energies what is equivalent to a distribution of z. Although this does not affect (practically) the final angles $\theta_x(E)$, it does affect the lateral deflections $x(E)$ (see factor $(z-z')^2$ in eq. (3)). Thus again, the correlation suffers.

In order to study the above distributions and the correlation of angles and distances we have simulated a proton shower with primary energy $E_0 = 10^{17}$ eV. This is practically the highest energy which can be fully simulated (without any thinning) in a reasonable time. As it was shown earlier [3] the angular, lateral and energy spectra of electrons do not depend (practically) on the primary particle energy (or its mass) once taken at the same level of shower development, at the same age s. Thus, the results presented below refer to large showers with any primary energy and mass. In this paper we present results concerning mainly levels close to the shower maximum, i.e. $s \cong 1$.

From the simulated sample we calculate the correlation coefficient κ of the two variables , the radial angle θ_r and r at $s = 0.95$, where θ_r is the projection of the particle angle on the z,r - plane (containing the shower axis and the vector $\vec{r}$). We obtain $\kappa \cong 0.35 \div 0.4$ for any of the electron energies, values smaller than in the case of the small angle scattering (0.87), but not small enough to claim an independence of the two variables. A clear demonstration of this dependence is Fig.1 where the mean angle $< \theta_r >$ is presented as function of the lateral distance r/r_M (in the Molière units) for $E > 22$ MeV. Also shown are the dispersions σ_{θ_r} and σ_{θ_t} - that of the tangential angle θ_t being the projection of the electron angle θ on the plane perpendicular to $\vec{r}$.

Our final aim is to use the electron distributions for accurate predictions of the Cherenkov flux from EAS. This flux (from each element of the shower path length) depends on the shower age s of this element (as the shape of the energy distribution depends on s only), on its height h above see level (as the Cherenkov threshold energy E_{th} depends on it) and, of course, on the total number of electrons there N. Thus, it is necessary to find the distributions $f(\vec{\theta}, r; E, s)$ for fixed electron energies E. Then, reconstructing a particular shower, the integration above $E_{th}(h)$ together with the Cherenkov yield, gives the distribution of the Cherenkov electrons. (An alternative way would be to find $f'(\vec{\theta}, r; s, h)$ for the Cherenkov electrons but the former distributions

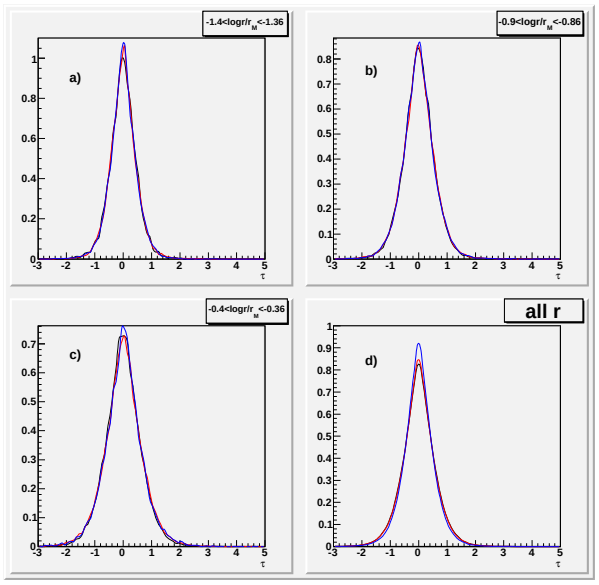

Figure 4: Distributions of $\tau = \theta_t \cdot E^{0.73}$ (θ in degrees, E in GeV) for three electron energies E =22 MeV (black curve), 67 MeV (red) and 200 MeV(blue)(from bins $(E, 1.1E)$); a) $-1.4 < y < -1.56$, b) $-0.9 < y < -0.86$, c) $-0.4 < y < -0.36$, d) all distances.

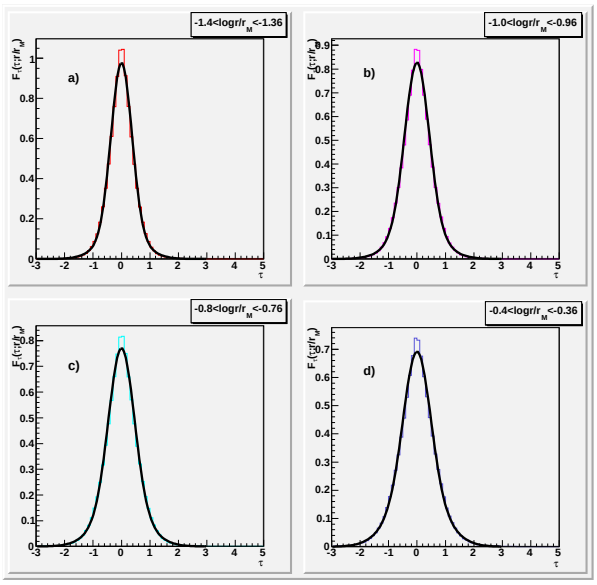

Figure 5: Distributions $F_\tau(\tau; r/r_M)$ (histograms) and fits with two Gaussians for distance bins as in Fig.3.

are independent of their later use (Cherenkov) and may be of a more general interest).

First we notice that the distributions of θ_r for different E (all r) scale in such a way that the distribution of $\rho = \theta_r \cdot E^\alpha$ is (almost) independent of E. For $s = 0.95$ we obtain $\alpha = 0.73$; its dependence on s being very weak. This is illustrated in Fig.2 where the distributions of $\rho = \theta_r \cdot E^{0.73}$ are presented for three electron energies (from the region where there are most of them) for all electron distances r. (However, α seems to decrease slightly with r, but at this stage we adopt it as independent of r.)

The value 0.73 can be understood as follows. From Eq.(2) it can be easily derived that

$$\sqrt{< \theta_r^2(E) >} \simeq \frac{E_s}{\beta} \sqrt{\frac{\beta}{E} - \ln(1 + \frac{\beta}{E})} \qquad (4)$$

if the electron energy loss rate for bremsstrahlung and ionisation equals (per unit path in cascade units) $-dE/dt = E + \beta$, and its initial energy $E_0 >> E$. In the energy region $0.2 \le E/\beta \le 2$, where there are most electrons, the r.h.s. of (4) can be very well approximated by $\sim E^{-0.73}$. As it turns out from simulations it is not only $\sqrt{< \theta_r^2(E) >} \cdot E^{0.73}$ that is independent of E, but (almost) also the distributions of θ_r (Fig.2)

Next we want to find the distributions of $\theta_r \cdot E^{0.73}$ for different r. A suitable function seems to be that of the Nishimura-Kamata form: $\beta^\mu / B(\mu, \nu - \mu) \cdot x^{\mu-1}(1 + \beta x)^{-\nu}$. Since θ_r (and ρ) may be negative we add to the variable ρ a value 3 deg $\cdot$ GeV$^{0.73}$ and fit the distributions of the above form with $x = \rho + 3$. The results are illustrated in Fig.3 where the actual distributions of $x = \theta_r \cdot E^{0.73} + 3$ are presented for electrons from four distance bins, together with the fitted curves. We see that the fits are quite good. (The fits with a gamma function were worse). The integrals over x of all distributions are equal to unity. The dependence of μ, ν and β on $y = log(r/r_M)$ have been parametrised as 3-degree polynomials: $a \cdot y^3 + b \cdot y^2 + c \cdot y + d$, and the coefficient values are given in Table 1.

There remain the distributions of the tangential angle θ_t. At this stage of analysis we assume that there is no correlation between θ_t and θ_r at a particular distance bin. Indeed, our study shows that the angular distribution (at a fixed r and energy E) depends (roughly) on $\eta = \sqrt{(\theta_r - < \theta_r >)^2 + \theta_t^2}$; if the distribution of η (per unit solid angle) was Gaussian (what is only approximately true) then the distributions of θ_r and θ_t would be independent.

We first check whether the distributions of $\tau = \theta_t \cdot E^{0.73}$ are independent of E, for each bin of $log(r/r_M)$. They are and the independence is even better fulfilled than that for $\rho = \theta_r \cdot E^{0.73}$. In Fig.4 we present the results for three values of E (as in Fig.2, three different colours) for three distance bins (a), b), c)) and for all r (d). Then we fit the distributions of τ for each distance bin with a sum of two Gaussian functions. Each fit has three free parameters: σ_1, σ_2 - the widths of each Gaussian and p - the weight of the first one (the both means are zero). The parameters have been parametrized as functions of $y = log(r/r_M)$ with 2-degree polynomials $b \cdot y^2 + c \cdot y + d$; the values of the coefficients are given in Table 1. In Fig.5 we compare the actual distributions of τ with the fitted functions for four distance bins. The fits are quite satisfactory.

Finally, at the considered level ($s = 0.95$) the number of electrons with energy $(E, E + dE)$ at a lateral distance $(r, r + dr)$ with angles $(\theta_r, \theta_r + d\theta_r)$ and $(\theta_t, \theta_t + d\theta_t)$ equals (with our approximations)

$$N \cdot f(\vec{\theta}, r; E, s) d\theta_r d\theta_t dr\, dE = \qquad (5)$$
$$\frac{\partial^2 N(r;E) dr\, dE}{\partial r \partial E} \cdot F_\rho(\theta_r E^{0.73} + 3; \frac{r}{r_M}) E^{0.73} \cdot d\theta_r \cdot$$
$$\cdot F_\tau(\theta_t E^{0.73}; \frac{r}{r_M}) E^{0.73} d\theta_t$$

where $F_\rho(x; \frac{r}{r_M}) = \beta^\mu / B(\mu, \nu - \mu) \cdot x^{\mu-1}(1 + \beta x)^{-\nu}$ and $F_\tau(\tau; \frac{r}{r_M}) = \frac{1}{\sqrt{2\pi}} [\frac{p}{\sigma_1} \cdot exp(\frac{-\tau^2}{2\sigma_1^2}) + \frac{(1-p)}{\sigma_2} \cdot exp(\frac{-\tau^2}{2\sigma_2^2})]$.

The lateral distribution for all angles $\frac{1}{N}\partial^2 N(r;E)/\partial E\partial r$ for electrons with fixed energies E has been shown to depend on r/r_M and s only [4] and parametrised there accordingly. N is the total number of electrons on the considered level and has to be taken from simulations as $< N(s) >$, or from the Gaisser-Hillas curve. $B(\mu, \nu-\mu)$ is the Euler beta function.

coeff → ↓parameter	a	b	c	d
μ	-	26.32	1.6	21.34
ν	0.0	0.0	0.0	171.0
β	-0.086	-0.044	-0.019	0.041
σ_1	-	-	0.138	0.905
σ_2	-	-0.092	-0.07	0.443
p	-	-	0.169	0.463

Table 1: Coefficients of the 3-degree polynomials ay^3+by^2+cy+d describing the parameters in the first column.

4 Shower image in the Cherenkov light

The UHECR experiments, like HiRes, Auger and TA, measure instantaneous optical images of showers propagating through the atmosphere. The fluorescence light dominates for most shower geometries (see e.g. [5]) but for viewing angles δ (the angle between the shower axis and the direction from the observed shower element to the telescope) smaller than $\sim 30^\circ$ the Cherenkov flux becomes important as well. If the shower is close enough so that its lateral extent can be measured by the telescope camera, the number of Cherenkov photons registered by an individual pixel of the camera will depend on the number of the emitting electrons at a particular lateral distance element seen by this pixel, having such angles so that the photons arrive to that pixel. Thus, the angular distribution of the emitting electrons has to be known as a function of their lateral distance. For distant showers (when all Cherenkov light falls into one pixel) one simply has that the Cherenkov signal is $\sim dN_{ch}(\delta)/d\Omega$, what is the angular distribution of all Cherenkov electrons (integrated over lateral distance r) but if more pixels are hit, the more accurate way to predict the Cherenkov flux (as above) should be applied.
To illustrate when the effect is important we have calculated the value of the Cherenkov signal produced at $s\sim 1$ and observed from two distances such that the total image is contained within angle ζ . Fig.6 presents the dependence of the signal as a function of the viewing angle δ calculated in an approximate way and accurately. The difference is better seen in Fig.7 where the ratio of the accurate to the approximate signal values is presented. We can see that even for $\zeta = 3.6^\circ$ the difference may be as big as $\sim 10\%$ or more.

5 Conclusions

Basing on a detailed simulation of 10^{17} eV showers we have worked out approximate formulae describing angular distribution of electrons as functions of their lateral distance and energy, close to shower maximum. We have also found that the distributions depend on $\theta\cdot E^\alpha$ (with $\alpha\cong 0.73$, explained in a simple way) rather than on θ and E separately.
Allowing for a correlation between the angular and lateral distributions is important in the reconstruction of shower characteristics from its optical images, particularly when the Cherenkov component is not to be neglected. The dependence on the shower age parameter s will be studied.

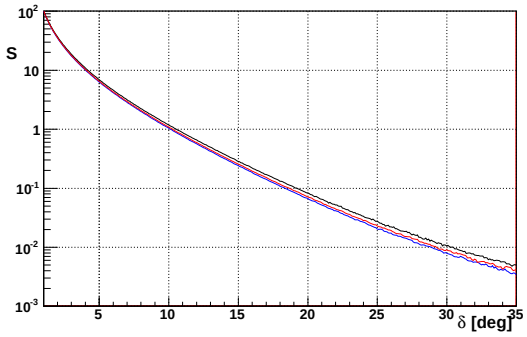

Figure 6: Cherenkov signal S (in arbitrary units) produced at shower maximum ($s\simeq 1$) (per unit solid angle) as function of viewing angle δ of the centre of its image with angular radius ζ. Approximate calculations ($S\sim dN_{ch}(\delta)/d\Omega$) - black curve, accurate ones for $\zeta = 3.6^\circ$ - red, $\zeta = 7.2^\circ$ - blue.

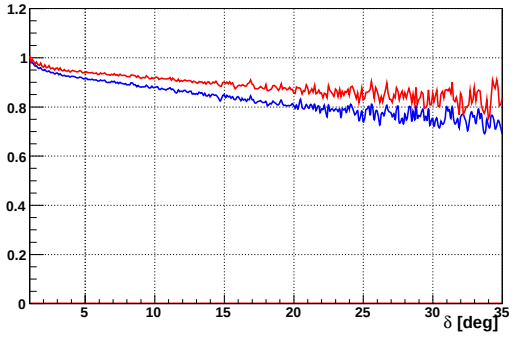

Figure 7: Ratio of the accurately calculated Cherenkov signal to the approximate one as function of δ, for $\zeta = 3.6^\circ$ - red, $\zeta = 7.2^\circ$ - blue.

Acknowledgment: The subject of the paper has been studied by us in connection with our participation in the Pierre Auger Collaboration and we thank the Collaboration for the discussions. The paper has been supported by the Polish NCN grant N N202 200239

References

[1] D. Heck et al. Report FZKA 6019 (Forschungszentrum Karlsruhe), 1998
[2] H. S. Snyder and W. T. Scott, Phys. Rev. 76 (1949) 220
[3] M. Giller et al. J. Phys. G Nucl. Part. Phys. 30 (2004) 97; M. Giller et al. J. Phys. G Nucl. Part. Phys. 31 (2005) 947; M. Giller et al. Int. J. Modern Phys. A 20 (2005) 6821
[4] M. Giller, A. Kacperczyk and W. Tkaczyk, Proc. ICRC2007, 4, 397 (ID 632)
[5] The Auger Collaboration, Nucl. Instr. Meth. A 523 (2004) 50